

Dielectric Relaxation Behavior of Conducting Carbon Black Reinforced Ethylene Acrylic Elastomer Vulcanizates

B. P. Sahoo,¹ K. Naskar,¹ R. N. P. Choudhary,² S. Sabharwal,³ D. K. Tripathy^{1,4}

¹Rubber Technology Centre, Indian Institute of Technology, Kharagpur 721302, West Bengal, India

²Ferroelectric Laboratory, Department of Physics and Meteorology, Indian Institute of Technology, Kharagpur 721302, West Bengal, India

³Radiochemistry and Isotope Group, Radiation Technology Development Section, Bhabha Atomic Research Centre, Trombay, Mumbai 400085, India

⁴Vice Chancellor, Veer Surendra Sai University of Technology, Burla 768018, Sambalpur, Odisha, India

Received 14 December 2010; accepted 8 June 2011

DOI 10.1002/app.35049

Published online 5 October 2011 in Wiley Online Library (wileyonlinelibrary.com).

ABSTRACT: The dielectric relaxation characteristics of conductive carbon black (CCB) reinforced ethylene acrylic elastomer (AEM) vulcanizates have been studied as a function of frequency (10^1 – 10^6 Hz) at different filler loading over a wide range of temperatures (30–120°C). The effect of filler loadings on the dielectric permittivity (ϵ'), loss tangent ($\tan \delta$), complex impedance (Z^*), and electrical conductivity (σ_{ac}) were studied. The variation of ϵ' with filler loading has been explained based on the interfacial polarization of the fillers within a heterogeneous system. The effect of filler loading on the imaginary (Z'') and real (Z') part of Z^* were distinctly visible, which may be due to the relaxation dynamics of polymer chains at the polymer–filler interface. The frequency dependency of

σ_{ac} has been investigated using percolation theory. The phenomenon of percolation in the composites has been discussed in terms of σ_{ac} . The percolation threshold (ϕ_{crit}) occurred in the range of 20–30 phr (parts per hundred) of filler loading. The effect of temperature on $\tan \delta$, ϵ' , σ_{ac} , and Nyquist plots of CCB-based AEM vulcanizates has been investigated. The CCB was uniformly dispersed within the AEM matrix as studied from the transmission electron microscope (TEM) photomicrographs. © 2011 Wiley Periodicals, Inc. *J Appl Polym Sci* 124: 678–688, 2012

Key words: elastomers; conducting carbon black; vulcanization; dielectric properties; dielectric percolation threshold

INTRODUCTION

The insulating rubber matrix can be converted into the conductive system by the incorporation of different types and appropriate amount of conductive fillers.¹ In general, fillers like metallic powders, flakes, whiskers, and other conducting fillers such as carbon black (CB), graphite, etc, were used for the development of electrically conducting polymer composites.² The CB filler forms the main ingredient for most of the rubber compounds. The conductive carbon blacks (CCBs) can be mixed with rubber and also may be handled like any other reinforcing or semi-reinforcing conventional CBs. It has been reported that strong interaction is an important parameter to optimize the properties of practical rub-

ber composites.³ Bound rubber (B_{DR}) experiments have been extensively used to measure the filler surface activity and filler–polymer interactions for many years. In general, B_{DR} content increases with higher loading of filler. At certain filler loading, the filler particles with polymer chain adsorbed on them which are not dispersed by the solvent and hence a coherent structure called polymer–filler gel was formed. The B_{DR} is strongly affected by the physico-chemical structure of filler and the rubber matrix. The CCBs are generally high structured and bulky in nature. The incorporation of sufficiently high loading of any types of CB imparts conductivity to the rubber compounds.⁴ However, the rubber composites exhibit electrical conductivity at very low CCBs loading. The loading changes the mechanical and electrical properties of the rubber materials. There is a tremendous scientific interest concerning the electrical properties of CB rubber composites. These materials are widely used for various electronic applications such as touch control switches for televisions, cameras, watches, variable volume control elements for electronic organs, and as strain sensors for various applications such as robot hands, artificial limbs, etc.

Correspondence to: D. K. Tripathy (dkt@rtc.iitkgp.ernet.in or vcvsut@gmail.com).

Contract grant sponsor: Board of Research in Nuclear Sciences (BRNS), Department of Atomic Energy (DAE), Mumbai, India; contract grant number: 2008/35/8/BRNS/3096.

CCBs are divided into two main categories: needle-shaped acetylene black and porous conductive black. Among them, the porous conductive black of hollow shell shape is better than the acetylene black from performance point of view as they induce conductivity more effectively with relatively less amount by increasing the net surface area.⁵

In this study, the porous Ketjen black EC300J CCB was used for preparation of acrylic elastomer (AEM) composites. Unlike conventional CBs, this CCB has very high surface area and high concentration of -OH functional groups on its surface, which in turn leads to high polymer–filler interactions.⁶ On increasing the surface area of CB, the number of rubber chain entanglement increases with the CB aggregates. One of the most important parameters of a given rubber compound reinforced with CB is the micro dispersion of the filler. This micro dispersion governs the fundamental properties of the composites. The electrical properties of CB filled rubber composites are greatly influenced by the state of dispersion as electrical conductivity measurement is an indirect method to assess the degree of dispersion of CB in the rubber matrix.⁷ The properties and performance of these composites are also affected by the degree of adhesion at the interface. The extent of adhesion at interface depends on the surface energy of the active functional groups and energetically different crystallite faces of the filler surfaces. The dielectric properties of these filled composites are widely varied according to aggregate size, surface area, and the conductivity of the filler particles. Development of conductive rubber composites based on electrical properties has gained a significant importance. The electrical properties of both CCB and short carbon fiber reinforced ethylene propylene diene monomer (EPDM) and EPDM/ethylene vinyl acetate (EVA) blend have been reported in literature.⁸ The percolation limit evaluated from the conductivity measurements for Ensaco 350G filled EPDM vulcanizates has been reported to be just above 40 phr loading.⁹ Mathew et al.¹⁰ reported the extensive study and cure kinetics of Cloisite 15A nanoclay based ethylene acrylate rubber (EAR) nanocomposites. However literature survey reveals that so far no work has been published regarding electrical characterization on AEM vulcanizates.

The prime objective of the present article is to develop conducting rubber composites using AEM and high surface area porous CCB (Ketjen black EC300J). The effect of filler loadings on dielectric properties (i.e., ϵ' , $\tan \delta$, Z^* , and σ_{ac}) as a function of frequency have been studied over a wide range of temperature. The percolation phenomenon has also been discussed as a function of filler loading.

TABLE I
Formulations of Unfilled and Ketjen EC300J Filled AEM Vulcanizates

Materials	Function	Phr
Ethylene acrylic Elastomer DP	Base rubber	100
Nuagard (MBPS)	Antioxidant	1.0
Stearic Acid	Processing aid	0.5
Vanfre VAM	Processing aid	0.5
Armeen 18D	Processing aid	0.5
Ketjen black (EC300J)	Conducting Filler	0, 10, 20, 25, 30, and 40
Vulcup TAC 70	Co-agent	2.0
Dicup 40C	Peroxide Curative	5

EXPERIMENTAL

Materials

Ethylene AEM dipolymer grade, commercially known as Vamac DP was obtained from DuPont Performance Elastomers, Wilmington, Delaware, USA. The Mooney viscosity ML (1 + 4) at 100°C is 22.0 (ASTM D1646-07). The conductive filler used in this study was highly conductive Ketjen EC 300J CCB having a N_2 surface area of 740–840 m^2/g , pH of 8–10, supplied by Akzo Nobel India Limited, India. The antioxidant Nuagard (MBPS) (4,4'-bis-(a,a'-dimethyl benzyl diphenylamine)) obtained from Chemtura Corporation, Philadelphia, Pennsylvania, USA. Di-Cup[®] 40C (40% dicumyl peroxide) and Vulcup TAC-70 (Triallyl cyanurate) used as curatives are obtained from Akzo Nobel India Limited. The processing aids (Stearic acid, Vanfre VAM (SEO) (complex of organic phosphate ester), Armeen18D (octadecyl amine)) were also obtained from Akzo Nobel India Limited.

Sample preparation

Preparation of AEM/CCB vulcanizates

The compound formulation is presented in Table I. The mixing of rubber with all other ingredients was carried out in a two-roll mixing mill (325 mm × 150 mm) at a friction ratio of 1 : 1.19 as per the ASTM D3182-07 standards with optimized temperature, nip gap, mixing time, and uniform cutting operation. A rubber process analyzer (RPA) was employed to determine the curing characteristics of the compounds. The compounds were cured for a fixed time of 19 min at 160°C and at an adequate pressure of 10 MPa.

The vulcanization process was carried out as per the optimum curing time (90% of the maximum curing time) using different conditions determined from torque data obtained from RPA. The compression-molded sheets were rapidly cooled by pouring them

into a water bucket at the end of the curing cycle. The sample sheets were conditioned for about 24 h before testing and characterizations. A fixed circular size sample having diameter of 12.18 mm and thickness of 2 mm was punched from the conditioned AEM vulcanizate sheets for dielectric measurements. The unfilled vulcanizate is represented as AEM and filled vulcanizates are designed as AEMX, where "X" stands for 10, 20, 25, 30, and 40 phr conductive Ketjen EC 300J CB.

Dielectric relaxation spectroscopy

The dielectric and electrical properties of the CCB-reinforced AEM vulcanizates were obtained using a computer-controlled impedance analyzer (PSM 1735) (N4L) on application of an alternating electric field across the sample cell with a blocking electrode (aluminum foil) in the frequency range of 10–10⁶ Hz at different temperatures (30–120°C). The parameters like ϵ' and dielectric $\tan \delta$ were obtained as a function of frequency and temperature. The σ_{ac} was calculated from the dielectric data using the following relation:

$$\sigma_{ac} = \omega \epsilon' \epsilon_0 \tan \delta \quad (1)$$

where ω is equal to $2\pi f$ (f is the frequency), and ϵ_0 is vacuum permittivity and ϵ' dielectric permittivity which is determined as:

$$\epsilon' = C_p / C_o \quad (2)$$

where C_p is the observed capacitance of the sample in parallel mode and C_o is the capacitance of the cell. The value of C_o is calculated using the expression $(\epsilon_0 A) / d$, where "A" and "d" are the area and thickness of the sample, respectively.

Bound rubber

Bound rubber content of the compound was determined by extracting the unbound materials such as ingredients and free rubber with toluene for 7 days, followed by drying for 2 days at room temperature. The weights of the samples were measured before and after the extraction, and the bound rubber content (B_{dR}) was calculated with the following expression:

$$B_{dR} = \frac{W_{fg} - W_t(m_f/m_f + m_r)}{W_t(m_f/m_f + m_r)} \quad (3)$$

where B_{dR} is the bound rubber content, W_{fg} is the weight of the filler and gel, W_t is the weight of the sample, m_f is the fraction of the filler in the compound, and m_r is the fraction of the rubber in the compound.

High-resolution transmission electron microscope

The distribution of CCBs into the AEM matrix was studied using a high-resolution transmission electron microscope (HRTEM) (JEM 2100, JEOL Limited, Japan) attached with charge couple device (CCD) camera (Gatan, Inc., Pleasanton, California, USA) at an acceleration voltage of 200 keV. The samples for HRTEM analysis were prepared using an ultramicrotome (Ultracut UCT, Leica Microsystems GmbH, Austria). Freshly sharpened diamond knives with cutting edges of 45° were used to obtain cryosections of 50–70 nm thick specimens at ambient temperature of –90°C, which is well below the T_g of the AEM rubber.

RESULTS AND DISCUSSION

Dielectric relaxation spectroscopy

The dielectric relaxation spectroscopy (DRS) provides information about the segmental mobility of the polymer by probing its dielectric properties. The testing frequencies in DRS corresponding to the broad range of relaxation times were associated with the polymer chains. Relaxation in filled elastomer is time-, temperature-, and frequency-dependent. It reflects the same chain motions as the mechanical modulus. However, it has reduced interference due to symmetry from shorter time processes. The frequencies of testing in DRS correspond to the extraordinarily broad range of relaxation time associated with the polymer chains.

Dielectric permittivity

The dielectric permittivity (ϵ') shows the ability of a material to store electric potential energy under the influence of an external electric field, which is proportional to the capacitance and measures the alignment of dipoles. Figure 1(a) shows the variation of ϵ' as a function of applied frequency for unfilled and Ketjen EC300J reinforced AEM vulcanizates at room temperature (30°C). It is observed from Figure 1(a) that ϵ' continuously decreases with frequency and reaches at a constant value at about 10⁵ Hz. A rapid decrease in ϵ' may be noticed in a frequency range of 10–10³ Hz. The decrease in ϵ' on increasing the frequency is well expected in most of the dielectric materials. This may be attributed to the tendency of dipoles in macromolecules to orient themselves in the direction of the external alternating electric field and the uniform dispersion of the filler aggregates in the polymer matrix. At low frequency region, the degree of interfacial polarization is very high as compared to the high frequency range, which may be developed due to the heterogeneity in the rubber composites. However, in the high frequency range the dipole will hardly be able to orient themselves in

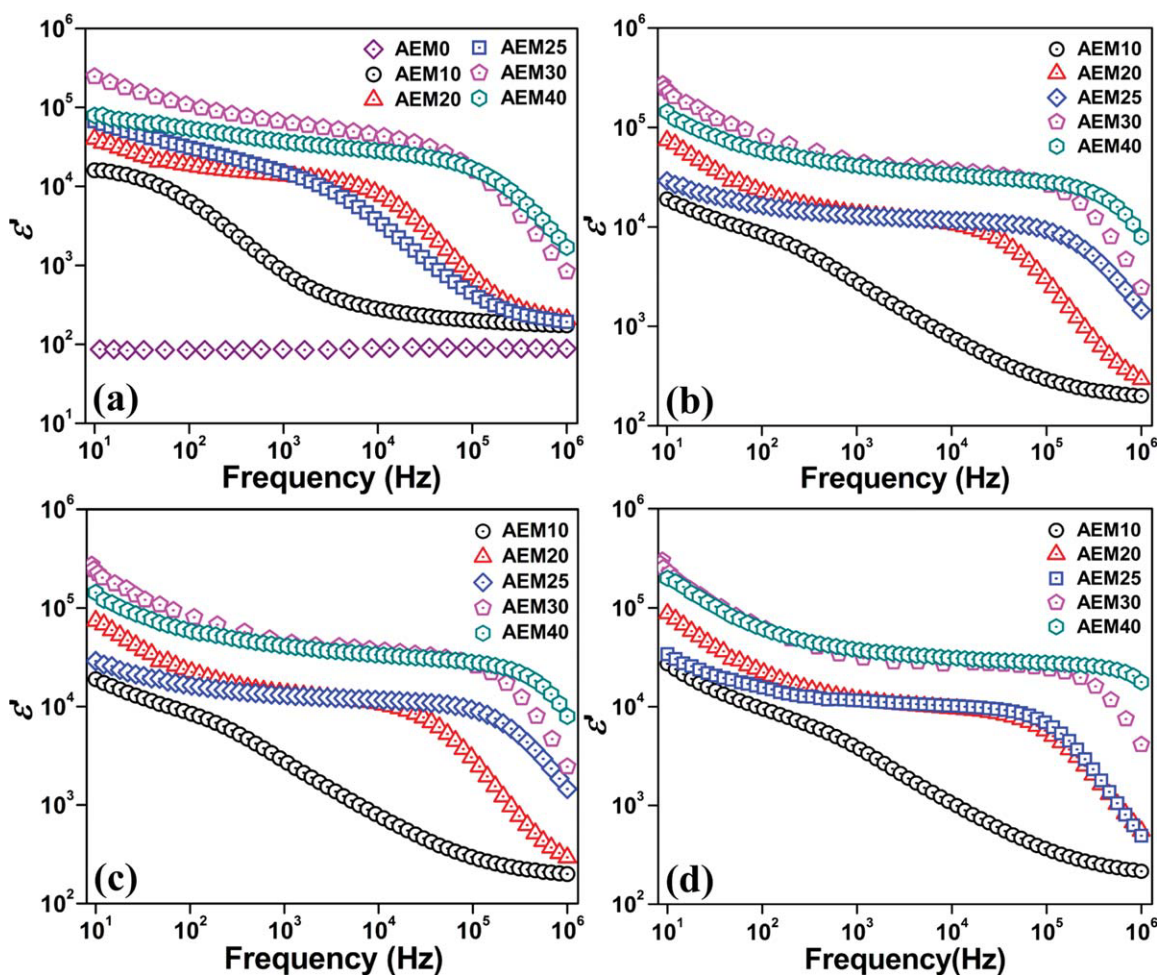


Figure 1 Effect of filler loading and temperature on the dielectric permittivity (ϵ') of AEM vulcanizates with increasing frequency at (a) 30°C, (b) 70°C, (c) 100°C, and (d) 120°C. [Color figure can be viewed in the online issue, which is available at wileyonlinelibrary.com.]

the direction of applied field and get less time to orient themselves in the direction of alternating field. At high frequency the periodic alternation of applied electric field occurs, that results in the drastic reduction in the diffusion of dipoles in the field direction and space charge accumulation, which result in the decrease in the values of polarization as well as in the ϵ' value. The relaxations in cross-linked polymers mainly depend upon the polymer–filler interactions,¹¹ which lead to the formation of an interphase. The thickness of the interphase is inversely proportional to the interfacial tension between viscoelastic polymer and solid filler phases. Increase in ϵ' with increase in concentration of Ketjen black can be explained on the basis of the enhancement of interfacial polarization with increase in concentration of filler loading. The value of ϵ' of AEM vulcanizates with 30 phr filler loading is found to be increased significantly to a level much higher than that of the virgin AEM, which is due to the space charge polarization and the uniform distribution of the filler in the matrix. The degree of polarization of CB is

higher which causes extra polarization under applied electric field as a consequence the ϵ' increases significantly at 30 phr Ketjen black content.¹² At the highest filler loading (40 phr), the decrease in ϵ' is observed. This may be due to any accidental inclusion and inherent imperfection of polymer composites such as inhomogeneous dispersion. The surprise reduction in ϵ' is due to the restriction motion of polymer chain at higher filler loading.¹³ The interface between the primary particles of the different filler aggregates act as the main barrier to the electron flow in conductor–polymer systems.

Figure 1(b–d) represent the variation of ϵ' with the frequency for 10, 20, 25, 30, and 40 phr Ketjen EC300J of AEM vulcanizates at 70, 100, and 120°C. At low frequencies, the ϵ' value of the samples reached to a higher value with increase in temperature. On increasing the temperature, the ϵ' increases due to the increase in segmental mobility of the dipoles at higher temperature.¹⁴ The model proposed by Klason and Kubát¹⁵ based on crystallinity

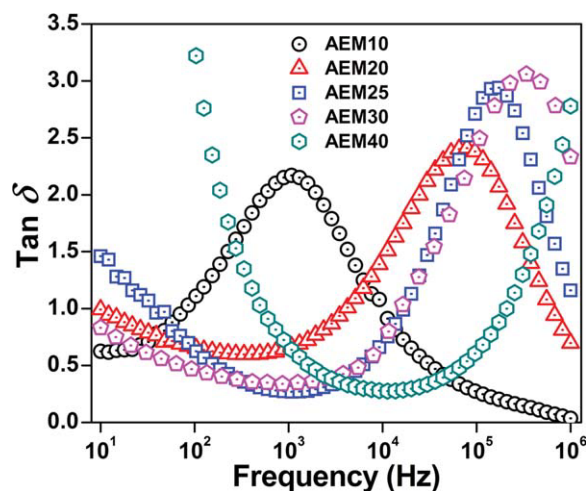


Figure 2 Variation of dielectric loss tangent ($\tan \delta$) as a function of frequency at 30°C for AEM vulcanizates with different filler loading. [Color figure can be viewed in the online issue, which is available at wileyonlinelibrary.com.]

suggested that at low temperature the CB structure was determined by crystalline phase of the polymer, distribution of CB particles in amorphous phase, and form conductive network chains. At higher temperature region, the structure is broken down that causes a more homogeneous distribution of particles as a result ϵ' is rapidly increased. It is also observed that the ϵ' value is gradually decreased with increase in frequency at all filler loading throughout the testing temperatures because dipoles did not get sufficient time to reorient themselves in the direction of external alternating electric field.

Dielectric loss factor ($\tan \delta$)

The loss factor is a parameter of a dielectric material that quantifies its inherent dissipation of electromagnetic energy. Figure 2 represents the variation of $\tan \delta$ with frequency for Ketjen C300J reinforced AEM vulcanizates at different filler loadings. The loss spectra were characterized by peak appearing at a characteristic frequency for the entire sample. It is clearly revealed that the $\tan \delta$ peaks shifted towards the higher frequency side with increase in filler load-

ing. This indicates that the relaxation time decreases on increasing the filler loading. The relaxation time of all the vulcanizates with different filler loadings are presented in Table II. The dielectric relaxation behavior of a polymer composite mainly depends upon the distribution of filler particles in the polymer matrix. Addition of functional fillers like CB not only results in hydrodynamic interactions but also leads to complex physico-chemical interactions between the polymer matrix and the filler surface.¹⁶ These elastomer–filler interactions are often characterized by the content of the apparent “bound rubber,” which is determined as the amount of insoluble rubber adhering to the dispersed CB aggregates before vulcanization. The bound rubber content can be considered as a measure of polymer–filler interactions, which mainly depends upon the surface area and the surface activity of fillers. CCB has very high surface area and contains high concentration of hydroxyl (-OH) functional groups, which lead to higher level of interactions in terms of hydrogen bonding with -COOCH₃ of the polymer matrix.¹⁷ The bound rubber content of CB filled unvulcanized rubber is increased with increase in filler loading, which is clearly observed from Table II. At highest filler loading (40 phr), no $\tan \delta$ peak is observed in the test frequency range (10^1 – 10^6). This is due to the decrease in mobility of the polymer chains in the vicinity of the filler surfaces.¹⁸ It is also found that the temperature largely affects the dielectric property of filled AEM vulcanizates. Figure 3 represents the frequency dependence of $\tan \delta$ for 20 phr loading of Ketjen EC300J reinforced AEM vulcanizates at different temperatures. It indicates that the relaxation time of AEM vulcanizates with 20 phr filler loading is decreased with increase in test temperature, which may be due to the thermal activation of the charge carriers.¹⁹

Impedance analysis

Electrical impedance extends the concept of resistance to AC circuits, describing not only the relative amplitudes of the voltage and current, but also the relative phases. The effect of filler loading on real

TABLE II
Bound Rubbers, Bulk Resistances (R_B), and Centre Positions [from Fig. 4(a)] of Ketjen EC300J Reinforced AEM Vulcanizates

Sample codes	Bound rubber (B_{dR}) (%)	Standard deviation of B_{dR}	R_B (Ω)	Centre position ($x, 0$)	Relaxation time (sec)
AEM10	15	0.5	1.6×10^6	$10.5 \times 10^5, 0$	9.25×14^{-4}
AEM20	33	1.5	3.5×10^5	$15.5 \times 10^4, 0$	1.419×10^{-5}
AEM25	34	0.8	2.5×10^5	$12.5 \times 10^4, 0$	6.265×10^{-6}
AEM30	41	0.8	8.5×10^4	$4.25 \times 10^4, 0$	7.042×16^{-6}
AEM40	53	0.7	4.5×10^4	$2.5 \times 10^4, 0$	–

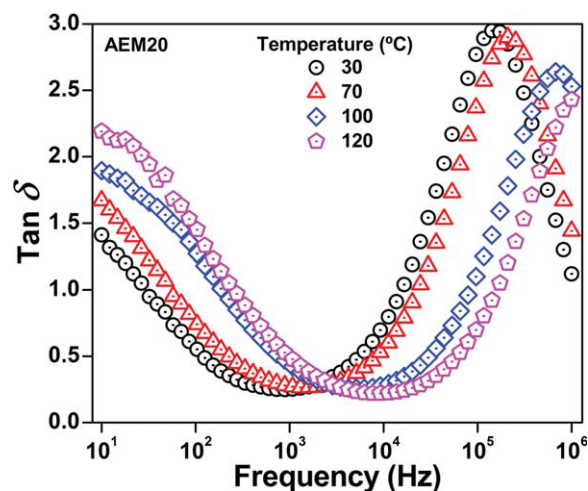


Figure 3 Variation of dielectric loss tangent ($\tan \delta$) as a function of frequency at different temperature for AEM20 vulcanizate. [Color figure can be viewed in the online issue, which is available at wileyonlinelibrary.com.]

part of impedance in AEM vulcanizates is shown in Figure 4(a). The complex impedance ($Z^* = Z' + jZ''$), where $j = \sqrt{-1}$ is the imaginary unit, and Z' and Z'' are real and imaginary parts of the Z^* , respectively. Z' accounts for the capacitance (storage of charge) of the system, whereas Z'' represents the loss factor (loss of accumulated charges, the conductive component) of the system.

The magnitude of Z' is gradually decreased for all the filled samples with increase in frequency and filler loading. This can be explained on the basis of the frequency-dependent relaxation phenomenon of cross-linked vulcanizates. Relaxation phenomenon in cross-linked and reinforced polymers depends on the chemical and physical interactions between the viscoelastic polymeric phase and solid filler phase. These interactions usually lead to the formation of interphase. This interphase quantified as " B_{dR} ," which in turn plays an important role in all polymeric system in bulk state. Because of the high surface area of the CCB (Ketjen EC300J), the polymer-filler interaction is very high, which leads to the formation of strong interphase. The interphase formed between the filler and polymer has distinct properties. Polymer layers having higher stiffness than that of bulk polymer in the vicinity of the dispersed phase surface is created from hindered molecular mobility because of the interfacial interactions.²⁰ Apart from this, the electron hopping is also an important mode of conduction, which becomes more significant in microwave frequency.²¹ It is well known that the conduction of current in conductive composites is mainly through the continuous conductive network, which is formed due to the homogeneous distribution of aggregated and agglomerated conductive fillers within the insulating

rubber matrix. This is reflected in continuous decrease in Z' with increasing frequency.²² The same argument can be extended to the variation in Z'' of impedance with frequency as shown in Figure 4(b) for different filler loading. From Figure 4(b), it is very much clear that Z'' decreases with frequency in the range of 10^1 – 10^5 Hz. This behavior can be attributed to the similar dielectric relaxation process of all the composites same as Z'' is related to the loss factor of the system.¹²

Nyquist plots

The Nyquist plots are generally the complex plane diagram of the Z^* . In this curve, Z' and Z'' are plotted along ordinate and abscissa, respectively. In fact, the Nyquist plot has a great similarity with well known Cole–Cole plot used to define the dielectric characteristics of materials. The effect of variation in filler loading on Nyquist plot is shown in

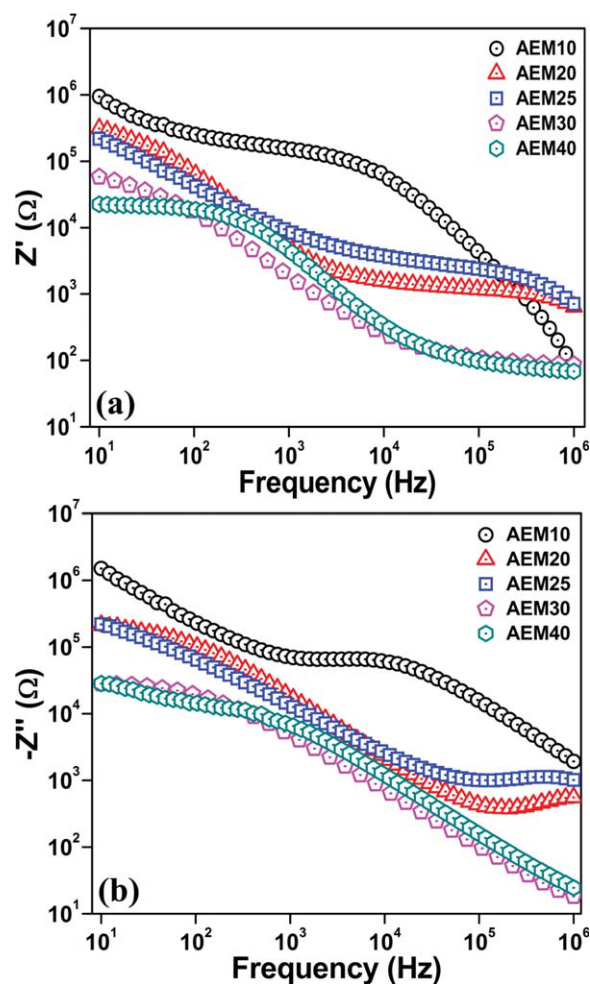


Figure 4 Variation of (a) Z' and (b) Z'' as a function of applied frequency at room temperature for AEM vulcanizates with different filler loading. [Color figure can be viewed in the online issue, which is available at wileyonlinelibrary.com.]

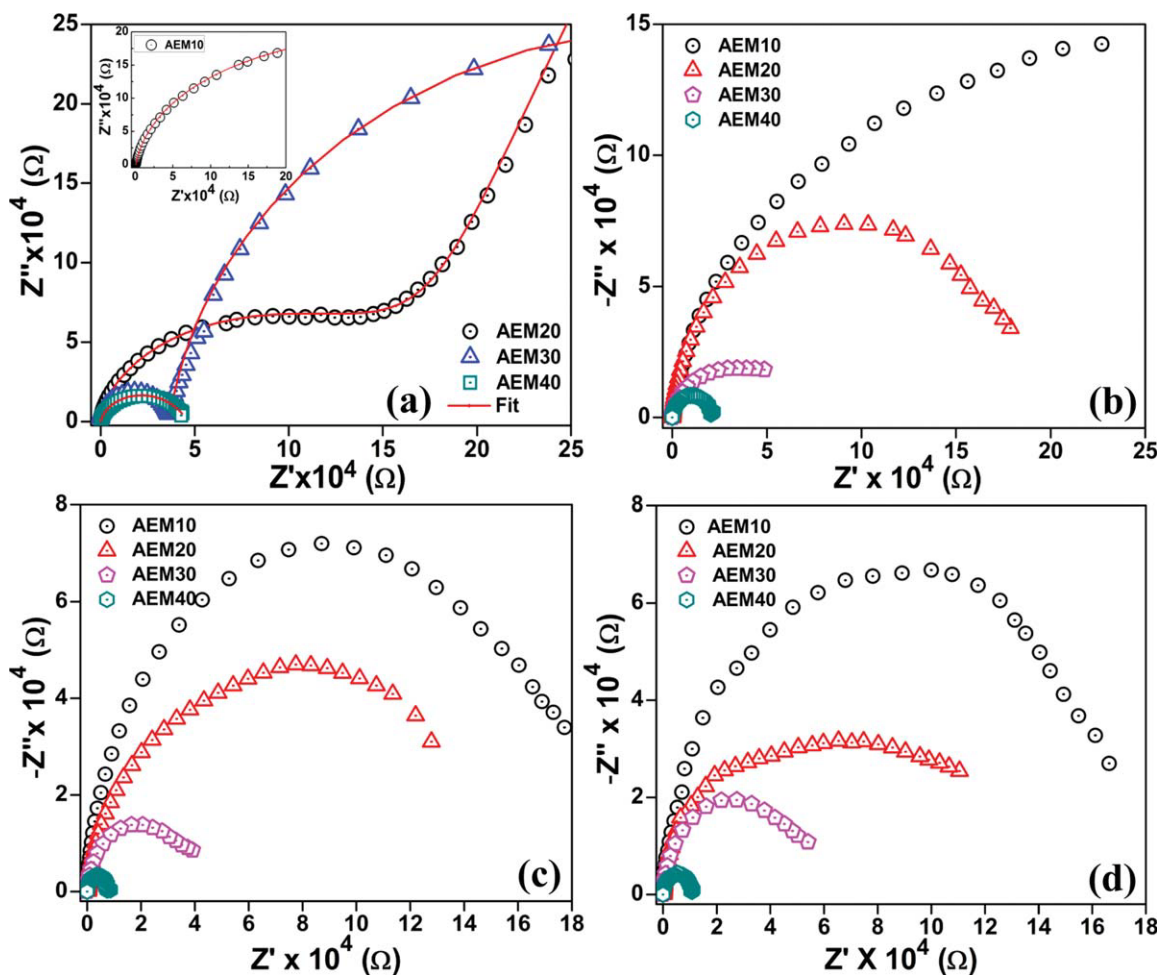


Figure 5 Nyquist plots (Z' vs. Z'') for AEM vulcanizates with different filler loading at (a) 30°C, (b) 70°C, (c) 100°C, and (d) 120°C. [Color figure can be viewed in the online issue, which is available at wileyonlinelibrary.com.]

Figure 5(a). It is noticed that the variation of CB loading has a sizable effect on the real and imaginary part of the impedance of the system. In Nyquist plot for polymer–composite system, the real part of impedance represents bulk resistance (R_B) and imaginary part of impedance represents maximum value of angular frequency (ω_{\max}), i.e., top of the semicircle, and is given by:

$$\omega_{\max} = 1/R_B C_B \quad (4)$$

The value of R_B is decreased with increase in filler loading, consequently the conductivity of the system significantly increased. However, with increase in filler loading there is a gradual improvement in bulk capacitance (C_B). It can be noticed in Figure 5(a) that with increase in filler loading the area under the semicircles of the Nyquist plot are getting reduced. The variation in values of radius and centre of semicircle can be used as a measure of gap in between the aggregates of CB particulates. The centre of the semicircle and R_B values for all filler loading have been given in Table II. It is observed from Table II

that with increase in filler loading, the R_B value is decreasing and at the highest filler loading the R_B is shifting from 1.6×10^6 to $4.5 \times 10^4 \Omega$. The centre of the semicircle also decreases. This may be due to increase in conductivity with increase in filler loading, which is in agreement with the conductivity plot (Fig. 6). The perfect semicircle is the characteristic of a single relaxation time system. The semicircular nature indicates the capacitive nature of the material (i.e., means the capacitive nature increases on increasing the filler loading). This phenomenon may be due to the formation of secondary structures (known as “aggregates”) resulting from the aggregation/agglomeration of the CB particulates.²³ With increasing filler loading, the distance between the aggregates reduces. The gap between the CB aggregates controls the electron conduction via non-Ohmic contacts between CB aggregates.

An equivalent circuit is commonly used to explain the impedance characteristics of the composites. Under an ideal condition, an equivalent circuit can be expected consisting of bulk resistance and parallel connected capacitance for semicircular regions.

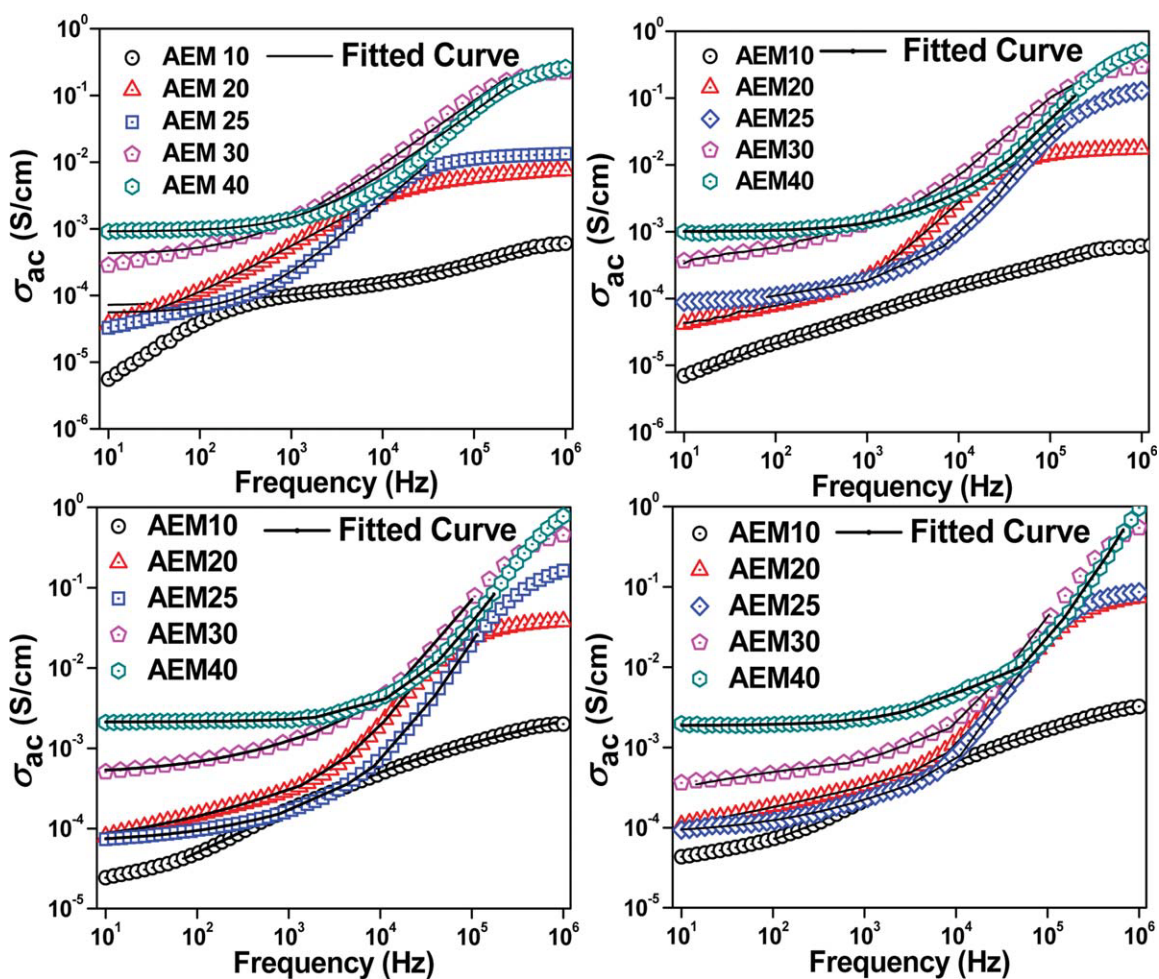
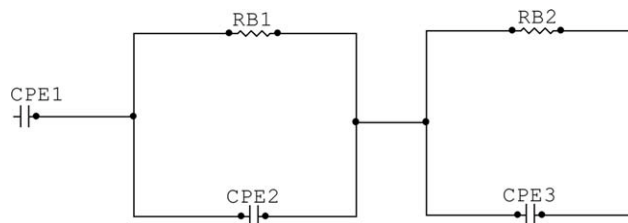


Figure 6 Variation of σ_{ac} with frequency and temperature for AEM vulcanizates with different filler loading at (a) 30°C, (b) 70°C, (c) 100°C, and (d) 120°C. [Color figure can be viewed in the online issue, which is available at wileyonlinelibrary.com.]

The obtained impedance data are correlated with the known equivalent circuits using electrochemical impedance spectroscopy (EIS) data analysis software (ZSimpWin) to design an equivalent circuit for the AEM/CCB vulcanizate system. Scheme 1 shows the proposed equivalent circuit for the AEM/CCB vulcanizates. In this equivalent circuit, three capacitances (CPE1, CPE2, and CPE3) are present instead of two bulk capacitances. When CPE is placed parallel to a resistor, a semicircle is produced. Here one semicircle is formed due to the parallel connection of CPE2 and RB1 and another semicircle may form at higher frequency region due to the parallel connection of CPE3 and RB2. CPE1 corresponds to the double layer capacity of inhomogeneous electrode surface.²⁴ The fitted curves [solid lines in Fig. 5(a)] show that the assumed equivalent circuit fits well with the experimental data. The bulk resistance and the capacitance along with the “*n*” values are tabulated in the Table III. The lower value of “*n*” represents the roughness of the electrodes.

Figure 5(a–d) shows the Nyquist plot at different temperatures. In this plot, the area under the semicircle gets reduced on increasing the temperature at all filler loading. This observation indicates that the R_B values of rubber vulcanizates decrease on increasing temperature, which is further confirmed by the conductivity plot at different temperatures. However, semicircular trend of the plots in vulcanizates indicates nonlinear nature of the polymer composites. Previous studies have shown that the CB particles dispersed in a polymer matrix are



Scheme 1 Electrical equivalent circuits for polarized conductive AEM/CCB vulcanizates.

TABLE III
Comparison of Parameters (Bulk Resistance, Capacitance, and “*n*” Values of CPE1, CPE2, and CPE3) Obtained from the Fitting of Experimental Data with the Equivalent Circuit [from Fig. 4(a)]

Sample codes	C_{CPE1} (F)	n_{CPE1}	C_{CPE2} (F)	n_{CPE2}	C_{CPE3} (F)	n_{CPE3}	RB1 (Ω)	RB2 (Ω)
AEM10	8.5×10^{-11}	0.99	4.1×10^{-8}	0.44	1.3×10^{-8}	0.85	1.2×10^{-1}	2.4×10^5
AEM20	8.5×10^{-10}	0.8	5.3×10^{-7}	0.52	1.8×10^{-8}	0.92	3.2×10^{-3}	1.4×10^3
AEM30	1.7×10^{-6}	0.22	6.8×10^{-11}	0.10	2.4×10^{-8}	0.93	1.5×10^{-3}	3.9×10^1
AEM40	1.5×10^{-7}	0.61	2.1×10^{-8}	0.94	2.2×10^{-5}	0.42	8.7×10^{-4}	1.1×10^1

electrically charged by fixed adsorbed ions or polar molecules and are surrounded by small counter-charges of the polymer matrix that form an electrical double layer.²⁵ The medium frequency relaxation is caused primarily by interfacial polarization, which is due to the build-up of charges on boundaries/interfaces between materials.²⁶ Application of an external AC field causes polarization of large colloidal particles, and creates perturbation in a miniature double layer on each particle, which behaves like macroions.²⁷ Under the influence of an external electric field, the counter ions are redistributed along the surface of filler particles, and hence double layer is formed and polarized, leading to interfacial polarization and the resulting relaxation or dispersion. The magnitude of relaxation of these counter-ions is much larger than the relaxation due to orientation of dipoles.

Electrical conductivity

The variation of σ_{ac} with frequency for AEM vulcanizates at different filler loadings is shown in Figure 6(a). The bulk electrical conductivities σ_{ac} of the CCB filled rubber composites is enhanced with increase in filler loading. At higher filler loading, the σ_{ac} value significantly increases compared to that of the lower filler loading vulcanizates. Irrespective of the filler loading, the σ_{ac} value of AEM vulcanizates is predominantly increased with increase in frequency. The increase in σ_{ac} with frequency is more prominent in the frequency range of 10^4 – 10^6 Hz. The σ_{ac} of the CB filled rubber composites primarily depends on the degree of dispersion of filler particles throughout the rubber matrix. At low level of filler loading, the conductivity of composite is slightly higher than that of the base polymer. At lower CB loading, the conductivity of the rubber vulcanizates is exhibited primarily due to the hopping and tunneling mechanisms.²⁸ In this mode of conduction, the electron transport may still couple strongly with the molecular and ionic processes in insulating AEM matrix. The main reason for the frequency dependency of σ_{ac} of rubber composites is generally attributed to the hopping transport phenomena which arise in between localized sites. In most of the polymer composites, the functional rela-

tionship between the angular frequency (ω) and σ_{ac} is usually in accordance with the power law, which is mathematically represented as follow.

$$\sigma(\omega) \propto \omega^s \quad (5)$$

Where “*s*” is an exponent. The value of “*s*” reside in between 0 and 1 (i.e., $0 \leq s \leq 1$) but in most cases “*s*” is nearly equal to unity. Hence, σ_{ac} is frequency dependent but DC conductivity is independent of frequency.²⁹ It is noted that the overall frequency dependence of σ (called universal dynamic response) of the σ_{ac} could be approximated led by the following relation:

$$\sigma_{\text{ac}} = \sigma_{\text{dc}} + A\omega^s \quad (6)$$

where “*A*” is a constant.

Power law fitting curves are shown in Figure 6(a–d). The solid lines in the graphs represent the fitted curves. The deviation from the DC conductivity (σ_{dc}) value in the conductivity plot in the low frequency region is due to the electrode polarization effect. The values of σ_{dc} , *A*, and *n* as obtained by fitting the power law equation are presented in Table IV. It is observed that σ_{dc} is increased with increase in CCB concentration in the AEM vulcanizates. It can be concluded that the continuous entangled network structure among filler aggregates is gradually increased with increase in filler loading, which forms a continuous conductive path for movement of charge particles within rubber matrix. Beyond a particular filler loading (≥ 20 phr), a sharp increase in σ_{ac} is observed which indicates the “percolation threshold limit.” At higher filler loading, the CBs are heterogeneous dispersed in the AEM matrix, which

TABLE IV
DC Conductivity Values Obtained from the Power Law Fitting Curves of the Conductivity Plots [from Fig. 5(a)]

Sample codes	σ_{dc} (S/cm)	<i>A</i>	<i>s</i>
AEM10	2.0×10^{-5}	1.9×10^{-6}	0.45
AEM20	3.0×10^{-5}	2.8×10^{-6}	0.75
AEM25	7.0×10^{-5}	2.9×10^{-7}	0.99
AEM30	4.2×10^{-4}	1.2×10^{-6}	0.96
AEM40	9.1×10^{-4}	5.7×10^{-9}	0.99

results in a broad distribution of hopping rate which causes a strong change in σ_{ac} .

Figure 6 (b-d) shows the plots of variation of the σ_{ac} with frequency for different filler loadings and temperatures (i.e., 70, 100, and 120°C). It is clearly observed from the figures that σ_{ac} increases with increase in temperature at all filler loadings, which confirms the negative temperature co-efficient (NTC) of resistance.³⁰ The increase in σ_{ac} with rise in temperature is mainly due to two phenomena: (a) thermal activation, which included the flocculation of particulate filler, leading to the formation of further conductive networks, (b) heating results an aerial oxidation process within the polymer matrix in presence of CB that forms polar carbonyl groups. Three main probable theories account for better understanding of the mechanism of electrical conduction through polymer composites, which are: (a) percolation theory, (b) electron tunneling theory, and (c) electric field radiation theory.

According to percolation theory,³¹ charged species move from one end to the other under an applied electric field through the conducting network, which is formed through physical contacts of conductive particles or their aggregates. In electron tunneling theory, conduction is by hopping or tunneling mechanism.³² According to electric field radiation theory, emission current flows by the high electric field, which is generated between the conducting elements separated by a gap of a few nanometers.¹⁴ According to percolation and electron tunneling theories, conduction in the polymer composite is ohmic in nature. The electric field radiation theory explains the non-ohmic conduction behavior for the present system.³³ At lower temperatures ($\leq 60^\circ\text{C}$), the contribution from conduction path or tunneling effect theory is more pronounced. At higher temperature ($\geq 60^\circ\text{C}$), the increased σ_{ac} is due to thermal activation, which is based on electric field radiation theory.

Dielectric percolation

The conductive filler forms a few continuous conductive networks in the polymer matrix through which charged species (electrons) move from one end to another end under an applied electric field. This movement of electrons causes the phenomenon of electric conduction. This is the basis of the well-known conduction path theory. Thus, the formation of conductive network through physical contacts of conductive particles or their aggregates is essential, and therefore, the formation of a conductive network is more probable above a critical value, which is known as percolation limit.

Figure 7 shows the effect of filler loading on the σ_{ac} of Ketjen EC300J reinforced AEM vulcanizates. At low level of CCB loading (10 phr), the σ_{ac} value

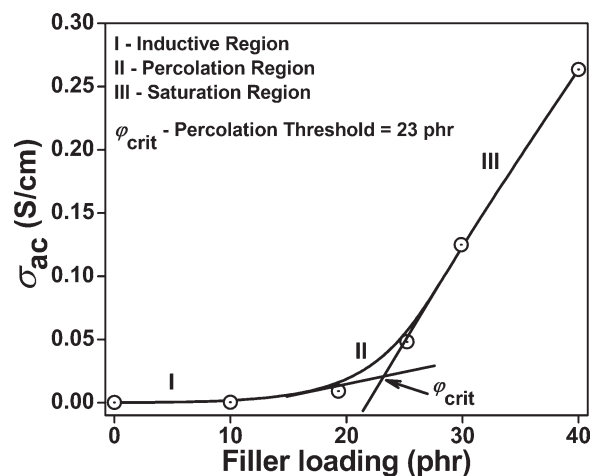


Figure 7 Variation of σ_{ac} with filler loading for AEM vulcanizates.

of the AEM composite is almost identical to the unfilled AEM vulcanizate. At lower CB loading, the interfacial distance between the CB aggregates is very high, as a consequent the movement of electrons is restricted within the rubber composites. In case of Ketjen black reinforced polymer composites, percolation limit has been observed at around 20 phr filler loading, which depends on the filler characteristics (i.e., surface area, surface activity, particle size, etc). The σ_{ac} of a polymer composite is normally characterized by its dependence on the filler volume fraction. At percolation threshold or critical loading level, the σ_{ac} of the rubber composites substantially increased where the volume fraction of conducting CB is sufficient enough to provide continuous path. The conducting elements of this path is either due to physical contact between them or separated by very small distances across which electron can tunnel. In the Ketjen EC300J filled AEM vulcanizates system, the percolation limit occurred just above 20 phr filler loading. It is found from the literature that the variation of σ_{ac} of CCB filled AEM composites may be divided into three parts: (i) inductive region: a small decrease in resistivity with filler loading which is due to the transportation of the small number of charged particles through the system without having any continuous conductive network; (ii) percolation region: the conductivity sharply increases due to the formation of continuous conductive path in the polymer matrix; (iii) saturation region: the marginal effect on σ_{ac} due to further addition of conducting filler. The percolation phenomenon may be of lattice percolation or continuum percolation. This involves two processes: randomly adding or removing particles from a simple lattice space until an infinite cluster is not formed. It has been recognized that the σ_{ac} of polymer composites

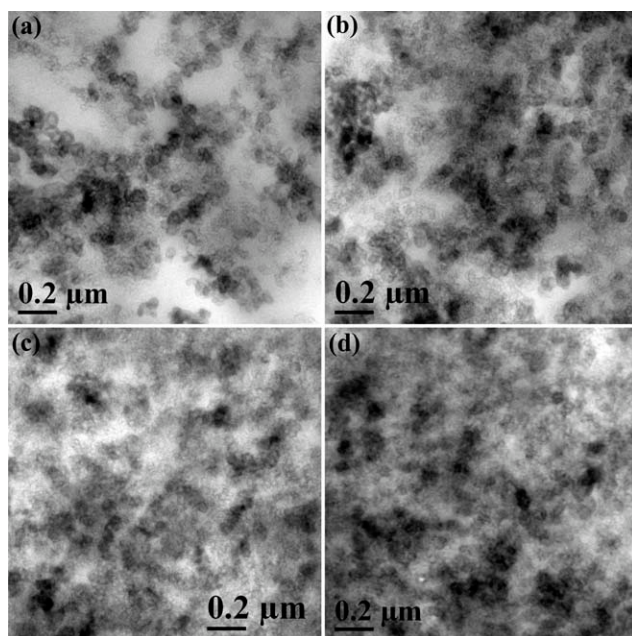


Figure 8 HRTEM microphotographs of AEM vulcanizates filled with (a) 10 phr, (b) 20 phr, (c) 30 phr, and (d) 40 phr of CCB.

not only depends on the geometry of filler particles but also on the processing of the materials.³⁴

High-resolution transmission electron microscope

Transmission electron microscope (TEM) photomicrographs of the CCB filled AEM composites are shown in Figure 8. TEM images revealed that the Ketjen EC300J is homogeneously dispersed within the polymer matrix. Beyond 20 phr CB loaded AEM composite, a continuous conductive path is developed due to close contact between the CB particles in the polymer matrix. This observation appears to be in good agreement with the electrical properties.³⁵

CONCLUSIONS

The dielectric relaxation of Ketjen EC 300J reinforced AEM vulcanizates has been studied as a function of variation in filler loading in the frequency range of 10^1 – 10^6 Hz at different temperature (30–120°C). With increase in filler loading, an increase in ϵ' is observed which can be explained on the basis of the interfacial polarization of the fillers in the polymer matrix. The variation of $\tan \delta$ with filler loading can be explained on the basis of the viscoelastic nature of the composites. In Nyquist plots, the area under the semicircles is reduced with increase in filler loading. It was analyzed through the resistance–capacitance circuit. The percolation limit of the filler in the matrix was found to be in the range of 20–30 phr loadings. The effects of temperature on $\tan \delta$, ϵ' , σ_{ac} , and Nyquist plots have also been studied. The maximum $\tan \delta$ peak has been shifted towards higher frequency region with

increase in temperature which is due to thermal activation process. The Nyquist plots showed that the real part of the complex impedance decreased with increase in temperature. This has been explained on the basis of conduction mechanism. TEM images revealed that the CB particles at low filler loading were homogeneously distributed in the AEM matrix, whereas beyond 20 phr filler loading, CB particles formed agglomerates within the rubber matrix.

References

1. Pramanik, P. K.; Khastgir, D.; De, S.; Saha, T. N. *J Mater Sci* 1990, 25, 3848.
2. Ghosh, P.; Chakrabarti, A. *Eur Polym J* 2000, 36, 1043.
3. Sobhy, M. D.; Nashar, E. E.; Maziad, N. A.; *Egypt. J. Sol* 2003, 26, 241.
4. Sau, K. P.; Chaki, T. K.; Khastgir, D. *J Appl Polym Sci* 1999, 71, 887.
5. Boehm, H. P. *Carbon* 1994, 32, 759.
6. Arico', A. S.; Antonucci, V.; Minutoli, M.; Giordano, N. *Carbon* 1989, 27, 337.
7. Cembrola, R. J. *Polym Eng Sci* 1982, 22, 601.
8. Das, N. C.; Chaki, T. K.; Khastgir, D. *Carbon* 2002, 40, 807.
9. Mahapatra, S. P.; Sridhar, V.; Chaudhary, R. N. P.; Tripathy, D. K. *Polym Compos* 2007, 28, 657.
10. Mathew, G.; Rhee, J. M.; Lee, Y.-S.; Park, D. H.; Nah, C. *J Ind Eng Chem* 2008, 14, 60.
11. Psarras, C.; Manolakaki, E.; Tsangaris, G. M. *Compos A* 2002, 33, 375.
12. Ku, C. C.; Liepins, R. *Electrical Properties of Polymers: Chemical Principles*; Hanser Publishers: Munich, 1987.
13. Qiang Yuan, Q.; Wu, D. *J Appl Polym Sci* 2010, 115, 3527.
14. Ying, X.; Yuezhen, B.; Chiang, C. K.; Masaru, M. *Carbon* 2007, 45, 1302.
15. Klason, C.; Kubát, J. *J Appl Polym Sci* 1975, 19, 831.
16. Mahaling, R. N.; Kumar, S.; Rath, T.; Das, C. K. *J Elastomers Plast* 2007, 39, 253.
17. Khatua, B. B.; Das, C. K. *J Appl Polym Sci* 2001, 80, 2737.
18. Nanda, M.; Chaudhury, R. N. P.; Tripathy, D. K. *Polym Compos* 2010, 31, 152.
19. Psarras, G. C.; Manolakai, E.; Tsangaris, G. M. *Compos A* 2003, 34, 1187.
20. Karásek, L.; Sumita, M. *J Mater Sci* 1996, 31, 281.
21. Mohanraj, G. T.; Chaki, T. K.; Chakraborty, A.; Khastgir, D. *Polym Eng Sci* 2006, 46, 1342.
22. Mahapatra, S. P.; Sridhar, V.; Tripathy, D. K. *Polym Eng Sci* 2007, 47, 984.
23. Deng, X.; Sridhar, V.; Mahapatra, S. P.; Kim, J. K. *J Appl Polym Sci* 2009, 111, 1358.
24. Pradhan, D. K.; Choudhary, R. N. P.; Samantaray, B. K.; Thakur, A. K.; Katiyar, R. S. *Ionics* 2009, 15, 345.
25. Balberg, I. *Carbon* 2002, 40, 139.
26. Verkoost, A. W. M.; Sluyters-Rehbach, M.; Sluyters, J. H. J. *Electroanal Chem Interfacial Electrochem* 1970, 24, 1.
27. Srivastava, N.; Chandra, S. *Eur Polym J* 2000, 36, 421.
28. Li, J.; Kim, J.-K. *Compos Sci Technol* 2007, 67, 2114.
29. Jäger, K.-M.; McQueen, D. H.; Tchmutin, I. A.; Ryvkina, N. G.; Klüppel, M. *J Phys D* 2001, 34, 2699.
30. Zhang, W.; Dehghani-Sanij, A. A.; Blackburn, R. S. *J Mater Sci* 2007, 42, 3408.
31. Jing, X.; Zhao, W.; Lan, L. *J Mater Sci Lett* 2000, 19, 377.
32. Halder, N. C. *Electrocomp Sci Technol* 1983, 11, 21.
33. Sau, K. P.; Chaki, T. K.; Khastgir, D. *J Mater Sci* 1997, 32, 5717.
34. Das, N. C.; Khastgir, D.; Chaki, T. K.; Chakraborty, A. *Compos A* 2000, 31, 1069.
35. Nanda, M.; Tripathy, D. K. *J Appl Polym Sci* 2010, 116, 2758.